

**Phenomenological analysis of rapidity distribution  
of negative pions in central  $^{12}\text{C}+^{12}\text{C}$  collisions  
at  $\sqrt{s_{nn}} = 3.14$  GeV**

Khusniddin K. Olimov<sup>\*,†,§</sup>, Qasim Ali<sup>\*</sup>, Mahnaz Q. Haseeb<sup>\*</sup>,  
Atif Arif<sup>\*</sup>, Sagdulla L. Lutpullaev<sup>†</sup> and B. S. Yuldashev<sup>‡</sup>

*\*Department of Physics,  
COMSATS Institute of Information Technology,  
Park Road, 44000 Islamabad, Pakistan*

*†Physical-Technical Institute of SPA,  
"Physics-Sun" of Uzbek Academy of Sciences,  
Bodomzor Yo'li Street 2b, 100084 Tashkent, Uzbekistan*

*‡Laboratory of High Energies,  
Joint Institute for Nuclear Research,  
RU-141980 Dubna, Russia  
§olimov@comsats.edu.pk*

Received 22 March 2015

Revised 19 May 2015

Accepted 20 May 2015

Published 10 June 2015

Various aspects of the simple phenomenological model, the grand combinational model (GCM), proposed earlier for the systematic description of the center-of-mass (cm) rapidity distributions of different particles produced in high energy heavy ion collisions, were analyzed. The values of GCM parameters were extracted from fitting the cm rapidity distributions of the negative pions in  $^{12}\text{C}+^{12}\text{C}$  collisions at  $\sqrt{s_{nn}} = 3.14$  GeV both in the experiment and using Modified FRITIOF Model. The GCM parameters extracted for the central  $^{12}\text{C}+^{12}\text{C}$  collisions were compared with those obtained in central Pb+Pb collisions at super proton synchrotron (SPS) and alternating gradient synchrotron (AGS) energies between  $\sqrt{s_{nn}} = 6.3$  GeV and  $\sqrt{s_{nn}} = 12.3$  GeV and in central Au+Au collisions at Relativistic heavy ion collider (RHIC) energies between  $\sqrt{s_{nn}} = 19.6$  GeV and  $\sqrt{s_{nn}} = 200$  GeV. The plausible physical interpretations for the GCM parameters were given. The initial assumption that the parameter  $\beta$  of GCM should be zero for symmetric systems with identical colliding nuclei was validated. The parameter  $\gamma$  of GCM was deduced to follow an approximate asymptotic behavior ( $\gamma \rightarrow 0$  as  $\sqrt{s_{nn}} \rightarrow \infty$ ) at very large cm energies, and  $\gamma \cong 0$  could possibly be related to complete dehadronization of the whole collision system, along with attaining its maximum possible energy density, in central collisions of identical nuclei. The behavior of cm energy

§Corresponding author.

dependence of  $\gamma$  suggested that it could possibly be sensitive to deconfinement phase transition.

*Keywords:* Central nucleus–nucleus collisions; symmetric collision systems; phenomenological analysis of rapidity distribution of hadrons; pions; dehadronization; deconfinement phase transition.

PACS Number(s): 14.40.Be, 25.10.+s, 21.65.Qr, 25.75.–q, 25.75.Nq

## 1. Introduction

The threshold energies for pion production in nucleon–nucleon collision are around 290 and 280 MeV for charged and neutral pions, respectively. Hence, pions are the predominantly produced particles in collisions of intermediate and high energy nuclei. The temperatures of pions, extracted from their transverse momentum or/and transverse energy spectra, are important for analysis of the nuclear equation of state. Pion production was also suggested as a probe of compressional energy in the high-density phase of near head-on collision.<sup>1,2</sup> Investigation of the properties of pions is also important for understanding the dynamics of a nuclear collision.

The pions produced at the energies of the Dubna synchrophasotron can be unambiguously separated from the other secondary particles produced in nuclear collisions. The excitation and decay of baryon resonances were shown to be one of the main processes responsible for pion production in relativistic nuclear collisions. In Refs. 3–11 it was shown that the significant fraction of pions produced in experiments on 2 m propane and 1 m hydrogen bubble chambers of the Joint Institute for Nuclear Research (JINR, Dubna, Russia) came from decay of delta resonances. It was stated also in Refs. 12–16 that the delta resonances play an important role in pion production in heavy ion collisions at the energies of the order of a few GeV/nucleon. The decay kinematics of  $\Delta$  resonances was shown to be responsible for the low transverse momentum enhancement of pion spectra in hadron–nucleus and nucleus–nucleus collisions at incident beam energies from 1 to 15 GeV per nucleon.<sup>4,15,16</sup>

Information about the state of excited and compressed nuclear matter, produced in relativistic nucleus–nucleus collisions, like collision dynamics and particle production mechanism could be extracted from analysis of the centrality dependence of the rapidity and transverse momentum spectra of pions.<sup>12,17–22</sup> The momentum, transverse momentum and rapidity distributions of the negative pions produced in Mg+Mg collisions at 4.3 GeV/c per nucleon were analyzed in Ref. 22. Analysis of pion rapidity distribution showed that the central rapidity region was occupied with pions of significantly larger transverse momentum as compared to the fragmentation region of interacting nuclei.<sup>22</sup> The rapidity distributions of negative pions in  $(p, d, \alpha, C) + C$  and  $(d, \alpha, C) + Ta$  collisions at 4.2A GeV/c were analyzed in different transverse momentum intervals of  $\pi^-$  in Refs. 20 and 21. With increasing transverse momentum, the fraction of negative pions in central rapidity region increased and the corresponding fraction in fragmentation region of colliding nuclei decreased.

Negative pions with large transverse momentum were mainly concentrated in central rapidity interval.<sup>20,21</sup> The quantitative analysis of centrality dependence of rapidity as well as that of transverse momentum spectra of the negative pions in  $d + {}^{12}\text{C}$ ,  ${}^{12}\text{C} + {}^{12}\text{C}$  and  ${}^{12}\text{C} + {}^{181}\text{Ta}$  collisions at  $4.2A\text{ GeV}/c$  was made in Ref. 23 by fitting the pion spectra with a Gaussian. The widths of rapidity spectra of  $\pi^-$ -mesons decreased in going from peripheral to central  $d + {}^{12}\text{C}$ ,  ${}^{12}\text{C} + {}^{12}\text{C}$ , and  ${}^{12}\text{C} + {}^{181}\text{Ta}$  collisions.<sup>23</sup> With increasing collision centrality, the centers of rapidity distributions of negative pions shifted towards the target fragmentation region in the case of asymmetric  $d + {}^{12}\text{C}$  and  ${}^{12}\text{C} + {}^{181}\text{Ta}$  collisions and remained at midrapidity position for symmetric  ${}^{12}\text{C} + {}^{12}\text{C}$  collisions. The extracted widths and mean values of transverse momentum versus rapidity spectra of negative pions did not depend within uncertainties on the masses of projectile and target nuclei as well as the collision centrality.<sup>23</sup>

It is necessary to add that the width of rapidity distribution of particles, produced in relativistic nucleus–nucleus collisions, contains information about the longitudinal flow<sup>24</sup> and final state rescattering.<sup>25</sup> Longitudinal flow was found to increase<sup>18</sup> with increasing  $\sqrt{s_{nn}}$ . For a given freeze-out temperature, the width of rapidity distribution in the Landau hydrodynamical model was found to be sensitive to the velocity of sound in the medium at freeze-out.<sup>26</sup>

The present paper is a continuation of our recent works,<sup>23,27–30</sup> which were devoted to analysis of the centrality dependence of rapidity and transverse momentum spectra of the negative pions along with their spectral temperatures in nucleus–nucleus collisions at  $4.2A\text{ GeV}/c$ . We will investigate various aspects of the simple phenomenological model, the grand combinational model (GCM),<sup>31–34</sup> via using it for description of the cm rapidity distribution of the negative pions in  ${}^{12}\text{C} + {}^{12}\text{C}$  collisions at  $4.2A\text{ GeV}/c$ . Following the expressions and ideas of Refs. 35–38 based on scaling properties of particle production, the GCM was developed and used<sup>31–34</sup> for the systematic description of the cm rapidity (pseudorapidity) distributions of various particles produced in central symmetric heavy ion collisions at high energies.

We will fit the cm rapidity distributions of the negative pions, produced in minimum bias, central, and peripheral  ${}^{12}\text{C} + {}^{12}\text{C}$  collisions at  $4.2A\text{ GeV}/c$  ( $\sqrt{s_{nn}} = 3.14\text{ GeV}$ ) by GCM. The GCM parameters extracted from fitting the cm rapidity distributions of the negative pions in central  ${}^{12}\text{C} + {}^{12}\text{C}$  collisions at  $\sqrt{s_{nn}} = 3.14\text{ GeV}$  will be compared with those obtained in Ref. 34 from approximation by GCM of the cm experimental rapidity (pseudorapidity) distributions of pions produced in central Pb+Pb collisions at SPS and AGS energies between  $\sqrt{s_{nn}} = 6.3\text{ GeV}$  and  $\sqrt{s_{nn}} = 12.3\text{ GeV}$  and in central Au+Au collisions at RHIC energies between  $\sqrt{s_{nn}} = 19.6\text{ GeV}$  and  $\sqrt{s_{nn}} = 200\text{ GeV}$ . Based on the analysis and comparison of our results with those obtained in high energy central heavy ion collisions, we aim to give a plausible physical interpretation of the GCM parameters lacking in Refs. 31–34. The applicability of GCM for adequate description of the experimental data from  ${}^{12}\text{C} + {}^{12}\text{C}$  collisions at intermediate energies will also be studied. For the sake of comparison, also the cm rapidity distributions of the negative pions, calculated

using Modified FRITIOF model adapted to intermediate energies,<sup>39–42</sup> in  $^{12}\text{C}+^{12}\text{C}$  collisions at  $\sqrt{s_{nn}} = 3.14 \text{ GeV}$  will be analyzed using GCM.

The paper is organized as follows. The experimental procedures and description of GCM are presented in Sec. 2. The analysis of the pion rapidity distributions using GCM and results are described in Sec. 3. Section 4 contains the summary and conclusions of the present work.

## 2. Experimental Procedures and GCM

The data analyzed in the present work were obtained using 2 m propane ( $\text{C}_3\text{H}_8$ ) bubble chamber of Laboratory of High Energies of JINR (Dubna, Russia). The chamber, placed in a magnetic field of strength 1.5 T,<sup>19,23,41,43–48</sup> was irradiated with beams of  $^{12}\text{C}$  nuclei accelerated to a momentum of 4.2 GeV/ $c$  per nucleon at Dubna synchrophasotron. Methods of selection of inelastic  $^{12}\text{C}+^{12}\text{C}$  collision events in this experiment were given in detail in Refs. 19, 23, 41 and 43–48. Threshold for detection of  $\pi^-$  mesons produced in  $^{12}\text{C}+^{12}\text{C}$  collisions was  $\approx 70 \text{ MeV}/c$ . In some momentum and angular intervals, the particles could not be detected with 100% efficiency. To account for small losses of particles emitted under large angles to object plane of the camera, the relevant corrections were introduced as discussed in Refs. 19, 23, 41 and 43–48. The average uncertainty in measurement of emission angle of the negative pions was 0.8 degrees. The mean relative uncertainty of momentum measurement of  $\pi^-$  mesons from the curvature of their tracks in propane bubble chamber was  $\approx 6\%$ . All the negative particles, except for those identified as electrons, were considered to be  $\pi^-$  mesons. Admixtures of unidentified electrons and negative strange particles did not exceed 5%. In our experiment, the spectator protons are: Protons with momenta  $p > 3 \text{ GeV}/c$  and emission angle  $\theta < 4$  degrees (projectile spectators) and protons with momenta  $p < 0.3 \text{ GeV}/c$  (target spectators) in the laboratory frame.<sup>19,23,41,43–48</sup> Thus, the participant protons are the protons which remain after elimination of the spectator protons. The statistics of the experimental data analyzed in the present work consists of 20,528  $^{12}\text{C}+^{12}\text{C}$  minimum bias inelastic collision events with practically all the secondary charged particles detected and measured in  $4\pi$  acceptance.

For the purpose of comparison, we simulated 50,000  $^{12}\text{C}+^{12}\text{C}$  minimum bias inelastic collision events using Modified FRITIOF model adapted to intermediate energies.<sup>39–42</sup> The model parameters used for simulation were the same as given in Ref. 40. Modified FRITIOF model could describe quite satisfactorily many results obtained in hadron–nucleus and nucleus–nucleus collisions at JINR experiments at intermediate energies.<sup>30,40–42,49,50</sup> The brief description of the model is given below.

The FRITIOF model assumes the two particle kinematics of inelastic  $hh$  interactions,  $a + b \rightarrow a' + b'$ , where  $a'$  and  $b'$  are excited states of initial hadrons  $a$  and  $b$ , respectively. The excited states are characterized by their masses. To choose hadron masses, the approach presented in Refs. 51 and 52 was employed. The

model parameters were refined in Refs. 53 and 54. In case of  $hA$  and  $AA$  interactions, it is assumed that nucleons excited in primary collisions can interact with each other and with other nucleons, and so their masses increase steadily with successive interactions. The probability of multiple scatterings was calculated using Glauber approach. Excited hadrons were considered as quantum chromodynamics (QCD) strings, and fragmentation of these strings resulted in production of hadrons. The multiplicity of secondary particles increased with increasing the string mass. To determine the time sequence of nucleon–nucleon collisions in case of  $hA$  and  $AA$  interactions, the Glauber approximation was used. Since cascade processes involving secondary particles were disregarded, the characteristics of slow particles produced in the breakup of a nucleus could not be described in the FRITIOF model. To overcome this drawback, it was suggested to modify FRITIOF model by supplementing it with the Reggeon model of a nucleus breakup.<sup>55</sup> The nucleus breakup was taken into account in two steps. In the first step, the number of inelastically interacting nucleons (that is, the number of the so-called hit ones) was determined using Glauber approximation.<sup>56</sup> In the second step, the noninteracting nucleons were considered. It was assumed that a noninteracting nucleon, which is at an impact distance  $r$  from a hit nucleon, can be involved in a Reggeon cascade with the probability  $W = C_{nd} \exp(-\frac{r^2}{r_{nd}^2})$ . Such a nucleon can involve another spectator nucleon, and so on and so forth. All the hit and involved nucleons were assumed to leave the nucleus. To describe adequately the multiplicity of protons participating in collisions of nuclei with carbon nuclei, the parameter values  $C_{nd} = 1$  and  $r_{nd} = 1.2$  fm were chosen. To calculate the excitation energy of the residual nucleus, the method presented in Ref. 57 was used. The evaporation model<sup>58,59</sup> was employed to simulate the relaxation of excited nuclei. The absolute normalization of the spectra was determined by the Glauber cross-sections. The center-of-mass (cm) correlations were accounted for as shown in Ref. 60. The densities of light nuclei were parameterized as given in Ref. 57. Modifications of the characteristics of  $NN$  interactions in a nuclear medium were not considered in the Modified FRITIOF model.

Comparison of the mean multiplicities per event of the negative pions and participant protons and the average values of rapidity and transverse momentum of  $\pi^-$  mesons in  $^{12}\text{C}+^{12}\text{C}$  collisions at  $4.2A$  GeV/ $c$  in the experiment and Modified FRITIOF model is presented in Table 1.

Table 1. Mean multiplicities per event of the negative pions and participant protons and the average values of rapidity and transverse momentum of  $\pi^-$  mesons<sup>30</sup> in minimum bias  $^{12}\text{C}+^{12}\text{C}$  collisions at  $4.2A$  GeV/ $c$  ( $\sqrt{s_{nn}} = 3.14$  GeV). The mean rapidities are calculated in cm of  $^{12}\text{C}+^{12}\text{C}$  collisions. Only statistical errors are given here and in the tables that follow.

Type	$\langle n(\pi^-) \rangle$	$\langle n_{\text{part. prot.}} \rangle$	$\langle y_{\text{c.m.}}(\pi^-) \rangle$	$\langle p_t(\pi^-) \rangle$ , GeV/ $c$
Experiment	$1.45 \pm 0.01$	$4.35 \pm 0.02$	$-0.016 \pm 0.005$	$0.242 \pm 0.001$
Mod. = Modified FRITIOF	$1.42 \pm 0.01$	$3.96 \pm 0.01$	$-0.017 \pm 0.003$	$0.248 \pm 0.001$

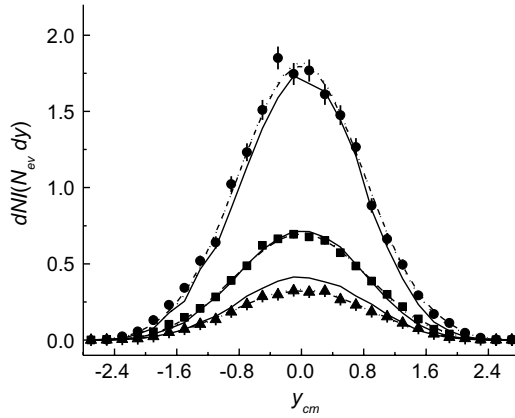


Fig. 1. The experimental cm rapidity distributions of the negative pions in central ( $\bullet$ ), peripheral ( $\blacktriangle$ ) and minimum bias ( $\blacksquare$ )  $^{12}\text{C}+^{12}\text{C}$  collisions at  $\sqrt{s_{nn}} = 3.14$  GeV along with the modified FRITIOF calculations (solid curves), and fits by the function in (4) for the fixed parameters  $\beta = 0, \Delta = 0.55$  (dotted curves) and for the fixed parameter  $\beta = 0$  only (dashed curves). All the spectra are normalized per one inelastic collision event.

As seen from Table 1, Modified FRITIOF model reproduced quite well the mean multiplicity, the mean cm rapidity, and the mean transverse momentum of the negative pions in experiment. As observed from Fig. 1, Modified FRITIOF model described satisfactorily the experimental rapidity distributions of  $\pi^-$  in minimum bias, central and peripheral  $^{12}\text{C}+^{12}\text{C}$  collisions at  $\sqrt{s_{nn}} = 3.14$  GeV. A fairly satisfactory agreement between the experimental and model rapidity distributions of the negative pions, as well as their average characteristics given in Table 1, indicates a practical absence of systematic uncertainties in experimental measurements of  $\pi^-$  in  $^{12}\text{C}+^{12}\text{C}$  collisions. Because the collision impact parameter cannot be measured directly, the number of participant protons,  $N_p$ , was used to characterize the collision centrality. References 19, 28, 29 and 61 were followed to define peripheral collision events to be those in which  $N_p \leq \langle n_{\text{part. prot.}} \rangle$  and central collisions as the collision events with,  $N_p \geq 2\langle n_{\text{part. prot.}} \rangle$ , where  $\langle n_{\text{part. prot.}} \rangle$  is the mean multiplicity per event of participant protons. It was shown in Ref. 61 that the central  $^{12}\text{C}+^{181}\text{Ta}$  collisions at  $4.2A$  GeV/c selected using the above criterion were characterized by complete projectile stopping, because, in these collisions, the average number of interacting projectile nucleons was very close to the total number of nucleons in a carbon projectile. The same criteria (as given above) were applied separately to the experimental data and Modified FRITIOF model data to determine the number of participant protons in each collision event and select the corresponding peripheral and central collision events in both the experiment and model. Fractions of the central and peripheral  $^{12}\text{C}+^{12}\text{C}$  collision events, relative to the total inelastic cross-section, obtained for both experimental and Modified FRITIOF model data are presented in Table 2. As seen from Table 2, the experimental and the corresponding model fractions of peripheral and central  $^{12}\text{C}+^{12}\text{C}$  collision events

Table 2. Fractions of central and peripheral  $^{12}\text{C}+^{12}\text{C}$  collision events at  $4.2A\text{ GeV}/c$  ( $\sqrt{s_{nn}} = 3.14\text{ GeV}$ ), relative to the total inelastic cross-section.

Peripheral collisions (%)		Central collisions (%)	
Experiment	Mod. = Modified FRITIOF	Experiment	Mod. = Modified FRITIOF
$58 \pm 1$	$62 \pm 1$	$11 \pm 1$	$12 \pm 1$

proved to be compatible with each other. Hence, as observed from Table 2, central  $^{12}\text{C}+^{12}\text{C}$  collision events, selected in the present work, corresponded to  $\sim (0-10)\%$  centrality, and the peripheral ones corresponded to  $\sim (40-100)\%$  centrality.

In Ref. 35, a working expression was formulated for phenomenological description of the cm rapidity distributions of particles in proton-proton collisions at Intersecting Storage Rings (ISR) energy ranges, given by a three-parameter expression

$$\frac{1}{\sigma} \frac{d\sigma}{dy} = \frac{dN}{N_{\text{ev}} dy} = C \left( 1 + \exp \frac{|y| - y_0}{\Delta} \right)^{-1}, \quad (1)$$

where  $C$  is a fitting constant,  $y_0$  and  $\Delta$  are two parameters,  $dN$  is the number of particles in the rapidity interval  $dy$ ,  $N_{\text{ev}}$  is the total number of inelastic collision events. The term on the left-hand side of Eq. (1) represents the rapidity density of particles normalized per one inelastic collision event. The choice of the above form was made to describe conveniently the central plateau and the fall off in the fragmentation region using the parameters  $y_0$  and  $\Delta$ , respectively. This relation was introduced also to check the concept of both the limiting fragmentation<sup>62</sup> and the hypothesis of Feynman scaling.<sup>63</sup> For all the five cm energies of proton-proton collisions at ISR, between  $\sqrt{s} = 23\text{ GeV}$  and  $63\text{ GeV}$ , the values of  $\Delta$  were extracted to be  $\sim 0.55$  for pions<sup>32</sup> and kaons,<sup>31</sup>  $\sim 0.35$  for protons/antiprotons,<sup>31</sup> and  $\sim 0.70$  for  $\Lambda$ ,  $\Xi$ ,  $\phi$ ,  $\Sigma$  and  $\Omega$ . These values of  $\Delta$  generally remained almost constant for the ISR cm energy range. Based on the fitting of the cm rapidity spectra of pions in proton-proton collisions at ISR energies, the energy dependence of the parameter  $y_0$  was observed<sup>32</sup> for pions to follow the empirical relationship

$$y_0 = 0.55 \ln \sqrt{s_{nn}} + 0.88. \quad (2)$$

Following the ideas and expressions of Refs. 35-38 on scaling properties of particle production, it was proposed to express the cm rapidity distributions of the particles produced in nucleus-nucleus collisions through Eq. (1), using the description of the cm rapidity spectra in proton-proton collisions, as follows:

$$\begin{aligned} \frac{dN}{N_{\text{ev}} dy} \Big|_{AB \rightarrow QX} &= C_1 (AB)^{f(y)} \frac{dN}{N_{\text{ev}} dy} \Big|_{pp \rightarrow QX} \\ &= C_1 (AB)^{\alpha + \beta y + \gamma y^2} \frac{dN}{N_{\text{ev}} dy} \Big|_{pp \rightarrow QX} \\ &= C (AB)^{\beta y + \gamma y^2} \left( 1 + \exp \frac{|y| - y_0}{\Delta} \right)^{-1}, \end{aligned} \quad (3)$$

where  $Q$  stands for the studied particle,  $X$  represents all the other products of the reaction.  $C_1$  and  $C = C_1(AB)^\alpha$  are the normalization constants,  $A$  and  $B$  are the mass numbers of the colliding nuclei, and  $\alpha, \beta$  and  $\gamma$  are the parameters to be extracted separately for each set of colliding nuclei  $A$  and  $B$  and cm energy. For the symmetric collisions with identical colliding nuclei ( $A = B$ ), the final working formula is expressed by

$$\left. \frac{dN}{N_{ev} dy} \right|_{AA \rightarrow QX} = C(AA)^{\beta y + \gamma y^2} \left( 1 + \exp \frac{|y| - y_0}{\Delta} \right)^{-1}, \quad (4)$$

which is the final expression for the symmetric collision systems in GCM. The above multiplicative factor  $(AA)^{\beta y + \gamma y^2}$  suggests that we could extract the physically meaningful parameters using expression (4) only for central collisions of identical nuclei, i.e., when practically all the nucleons of colliding nuclei participate in collision. The suggested choice of the function  $f(y) = \alpha + \beta y + \gamma y^2$  in expressions (3) and (4) was not accidental. The clue for such an expression was taken from the studies on the behavior of EMC effect in lepton–nucleus collisions, given in Ref. 64. Similar relationship was also used in Ref. 65 in a somewhat different context. The symmetric cm rapidity distributions of various particles produced in high energy collisions of identical heavy nuclei were analyzed using expression (4) in Refs. 33 and 34. Since the particles and collision systems analyzed in Refs. 33 and 34 substantially overlap, we will compare our results with those of the final analysis, given in Ref. 34. The coefficient  $\beta$  in expression (4) belongs to a term  $y$ , which is not symmetric under  $y \rightarrow (-y)$  transformation. Based on symmetry of the collision system, resulting in symmetric rapidity distribution, the  $\beta = 0$  was introduced<sup>33,34</sup> for the fits of cm rapidity distributions of various particles, produced in high energy collisions of identical nuclei.

### 3. Analysis and Results

The parameters extracted from  $\chi^2$  fitting by the expression in (4) of the experimental and Modified FRITIOF model cm rapidity distributions of the negative pions in minimum bias, central, and peripheral  $^{12}\text{C}+^{12}\text{C}$  collisions at  $\sqrt{s_{nn}} = 3.14 \text{ GeV}$  for the fixed  $\beta = 0$  and  $\Delta = 0.55$  and for the fixed  $\beta = 0$  only are presented in Tables 3 and 4, respectively.  $R^2$  factor in Tables 3 and 4 is given by relation  $R^2 = 1 - \frac{SS_E}{SS_T}$ , where  $SS_E = \sum_{i=1}^n (y_i^{\text{exp}} - y_i^{\text{fit}})^2$  is the sum of squared errors,  $SS_T = \sum_{i=1}^n (y_i^{\text{exp}} - \bar{y})^2$  is the total sum of squares,  $y_i^{\text{exp}}$  and  $y_i^{\text{fit}}$  are the original (experimental) and fit (model) data, respectively, and  $\bar{y} = \frac{1}{n} \sum_{i=1}^n y_i^{\text{exp}}$  is the mean value of the experimental data. As the deviation between the experimental and fit data gets smaller,  $R^2$  factor approaches to 1. Hence, the closer  $R^2$  factor value to 1, the better is the fit quality. The corresponding experimental and model cm rapidity distributions along with the two types of fits by the expression in (4) are shown in Figs. 1 and 2, respectively. It should be noted that the curves of these two types of fits mostly overlap in Figs. 1 and 2. As seen from Figs. 1 and 2, the experimental

Table 3. Parameters of approximation by the expression in (4) of the cm rapidity distributions of the negative pions in minimum bias, central and peripheral  $^{12}\text{C}+^{12}\text{C}$  collisions at  $\sqrt{s_{nn}} = 3.14$  GeV ( $\beta = 0, \Delta = 0.55$  are fixed).

Collision type	Type	$C$	$\gamma$	$y_0$	$\chi^2/\text{n.d.f.}$	$R^2$
Minimum bias	Experiment	$0.73 \pm 0.02$	$-0.13 \pm 0.03$	$2.06 \pm 0.71$	5.58	0.99
	Mod. = Modified FRITIOF	$0.76 \pm 0.02$	$-0.15 \pm 0.02$	$2.01 \pm 0.56$	7.61	0.99
Central $\sim (0-10)\%$	Experiment	$1.86 \pm 0.08$	$-0.14 \pm 0.04$	$2.16 \pm 1.10$	1.99	0.99
	Mod. = Modified FRITIOF	$1.80 \pm 0.11$	$-0.15 \pm 0.05$	$2.02 \pm 1.15$	1.97	0.99
Peripheral $\sim (40-100)\%$	Experiment	$0.34 \pm 0.03$	$-0.12 \pm 0.06$	$2.00 \pm 1.50$	1.79	0.99
	Mod. = Modified FRITIOF	$0.44 \pm 0.02$	$-0.14 \pm 0.04$	$2.00 \pm 0.91$	3.97	0.99

 Table 4. Parameters of approximation by the expression in (4) of the cm rapidity distributions of the negative pions in minimum bias, central and peripheral  $^{12}\text{C}+^{12}\text{C}$  collisions at  $\sqrt{s_{nn}} = 3.14$  GeV ( $\beta = 0$  is fixed).

Collision type	Type	$C$	$\gamma$	$y_0$	$\Delta$	$\chi^2/\text{n.d.f.}$	$R^2$
Minimum bias	Experiment	$0.69 \pm 0.01$	$-0.140 \pm 0.003$	$2.22 \pm 0.05$	$0.22 \pm 0.03$	2.72	0.99
	Mod. = Modified FRITIOF	$0.72 \pm 0.01$	$-0.152 \pm 0.005$	$2.08 \pm 0.08$	$0.33 \pm 0.04$	4.70	0.99
Central $\sim (0-10)\%$	Experiment	$1.80 \pm 0.03$	$-0.155 \pm 0.004$	$2.33 \pm 0.05$	$0.11 \pm 0.04$	1.12	0.99
	Mod. = Modified FRITIOF	$1.73 \pm 0.02$	$-0.166 \pm 0.008$	$2.26 \pm 0.13$	$0.31 \pm 0.10$	1.74	0.99
Peripheral $\sim (40-100)\%$	Experiment	$0.32 \pm 0.01$	$-0.127 \pm 0.008$	$2.10 \pm 0.11$	$0.26 \pm 0.06$	0.94	0.99
	Mod. = Modified FRITIOF	$0.41 \pm 0.01$	$-0.147 \pm 0.007$	$2.03 \pm 0.09$	$0.29 \pm 0.04$	1.72	0.99

and model cm rapidity distributions of the negative pions are described quite satisfactorily by the function in (4). It is necessary to mention that all the  $\chi^2$  fits of the present work were conducted by including the statistical uncertainties. The parameters extracted in Ref. 34 from  $\chi^2$  fitting by the expression in (4) of the cm experimental rapidity distributions of the negative pions in central Pb+Pb collisions at various SPS and AGS energies for the fixed  $\beta = 0$  and  $\Delta = 0.55$  are presented in Table 5, for a comparison.

As seen from Tables 3 and 4, the values of the fitting constant  $C$  proved to be significantly larger in case of central  $^{12}\text{C}+^{12}\text{C}$  collisions at  $\sqrt{s_{nn}} = 3.14$  GeV as compared to the peripheral ones both in the experiment and Modified FRITIOF model. Naturally, it reflected the physical fact that the mean multiplicity of the negative pions produced in central  $^{12}\text{C}+^{12}\text{C}$  collisions was considerably greater compared to that in peripheral ones. This is verified by the data of Table 6, which presents the mean multiplicities of the negative pions and their ratio along with the ratio of the extracted fitting constants  $C$ , given in Table 4, in central and peripheral  $^{12}\text{C}+^{12}\text{C}$  collisions at  $\sqrt{s_{nn}} = 3.14$  GeV. As seen from Table 6, the ratio of the fitting constants  $C$  in central and peripheral  $^{12}\text{C}+^{12}\text{C}$  collisions is

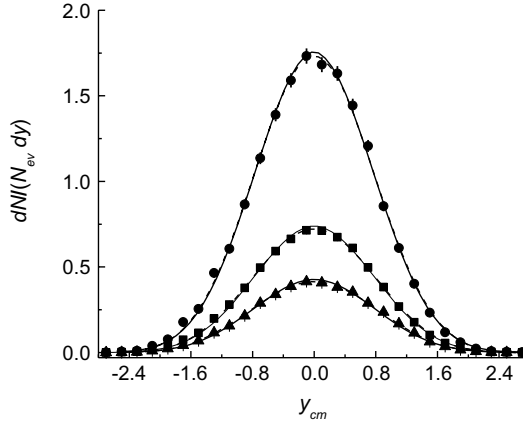


Fig. 2. The cm rapidity distributions of the negative pions, calculated using modified FRITIOF model, in central ( $\bullet$ ), peripheral ( $\blacktriangle$ ) and minimum bias ( $\blacksquare$ )  $^{12}\text{C}+^{12}\text{C}$  collisions at  $\sqrt{s_{nn}} = 3.14$  GeV along with the fits by the function in (4) for the fixed parameters  $\beta = 0, \Delta = 0.55$  (solid curves) and for the fixed parameter  $\beta = 0$  only (dashed curves). All the spectra are normalized per one inelastic collision event.

Table 5. Parameters extracted in Ref. 34 from approximation by the expression in (4) of the cm experimental rapidity distributions of the negative pions in central Pb+Pb collisions at various SPS and AGS energies ( $\beta = 0, \Delta \approx 0.55$ ).

$\sqrt{s_{nn}}$ (GeV)	6.3	7.6	8.7	12.3
$\gamma$	$-0.044 \pm 0.0003$	$-0.037 \pm 0.0003$	$-0.035 \pm 0.0003$	$-0.027 \pm 0.0002$

Table 6. Mean multiplicities of the negative pions and their ratios along with the ratios of the extracted fitting constants  $C$ , given in Table 4, in central and peripheral  $^{12}\text{C}+^{12}\text{C}$  collisions at  $\sqrt{s_{nn}} = 3.14$  GeV.

$\langle n(\pi^-) \rangle_{\text{central}}$	Experiment	$3.62 \pm 0.03$
	Modified FRITIOF	$3.33 \pm 0.02$
$\langle n(\pi^-) \rangle_{\text{peripheral}}$	Experiment	$0.70 \pm 0.01$
	Modified FRITIOF	$0.83 \pm 0.01$
$\frac{\langle n(\pi^-) \rangle_{\text{central}}}{\langle n(\pi^-) \rangle_{\text{peripheral}}}$	Experiment	$5.2 \pm 0.2$
	Modified FRITIOF	$4.0 \pm 0.1$
$\frac{C_{\text{central}}}{C_{\text{peripheral}}}$	Experiment	$5.6 \pm 0.2$
	Modified FRITIOF	$4.2 \pm 0.1$

compatible, within the uncertainties, with the ratio of the mean multiplicities of the negative pions in central and peripheral collisions, both in the experiment and model. This suggests that parameter  $C$  in expression (4) fixes the multiplicity of the studied particles. Tables 3 and 4 show that the values of  $C$  are compatible with each other in the experiment and model, whereas the extracted values of the parameter

$\gamma$  are lower in the model compared to experiment. As observed from Tables 3 and 4, the values of  $\gamma$  were extracted to be consistently lower in central  $^{12}\text{C}+^{12}\text{C}$  collisions as compared to the peripheral ones, both in the experiment and model. It is seen from comparison of Tables 3–5 that the value of  $\gamma$  proved to be consistently lower ( $\sim$  more than four times, on the average) in central  $^{12}\text{C}+^{12}\text{C}$  collisions at  $\sqrt{s_{nn}} = 3.14$  GeV as compared to central Pb+Pb collisions at various SPS and AGS energies  $\sqrt{s_{nn}} \geq 6.3$  GeV. This decreasing trend of  $\gamma$  with the decrease of  $\sqrt{s_{nn}}$  can also be seen for central Pb+Pb collisions in Table 5.

As noted from Tables 3 and 4, the parameters  $y_0(\gamma)$  and  $\Delta$  show some correlation, i.e.,  $y_0(\gamma)$  decreases (increases) weakly with the increase of  $\Delta$ . Let us recall that the parameters  $y_0$  and  $\Delta$  were introduced in expression (1) to describe conveniently the central plateau and the fall off in fragmentation region of cm rapidity distributions of produced particles in proton–proton collisions. Then, naturally,  $y_0$  could be associated with the quantity related to a rapidity spread (width) (around central rapidity region) in rapidity units of particles originated from expansion and freeze-out of a fireball. It was observed<sup>31,32</sup> for proton–proton collisions at ISR energies between  $\sqrt{s} = 23$  and 63 GeV that the energy dependence of  $y_0$  for pions,  $\Lambda$ ,  $\Xi$ ,  $\Sigma$ ,  $\phi$  and  $\Omega$  could be approximated empirically through the relation

$$y_0 = k \ln \sqrt{s_{nn}} + b, \quad (5)$$

where  $k$  was assumed to vary slowly with the cm energy, and  $b$  was a constant. Using empirical relation in (2), we obtained  $y_0 = 1.51$  for pions produced in proton–proton collisions at  $\sqrt{s_{nn}} = 3.14$  GeV, which proved to be lower than  $y_0$  values, extracted in the present analysis and given in Tables 3 and 4, for negative pions in central  $^{12}\text{C}+^{12}\text{C}$  collisions. This result can be understood if we recall that the width of the rapidity distribution of the produced particles should be larger in nucleus–nucleus collisions as compared to that in proton–proton collisions at the same  $\sqrt{s_{nn}}$ .

At lower energies (beam energies up to 10 GeV per nucleon on a fixed target, corresponding to  $\sqrt{s_{nn}} \leq 5$  GeV), it is expected that compressed nucleonic matter, or highly excited nuclear matter, with densities up to a few times the normal nuclear density ( $\rho_0 = 0.16$  GeV/fm<sup>3</sup>) and temperatures  $\sim 100$  MeV is produced in central nucleus–nucleus collisions.<sup>66–68</sup> In this case, only small fraction of the cm energy goes to production of new particles, such as pions and kaons, while the dominant fraction of the cm energy is carried away by the constituent nucleons of the colliding nuclei. This scenario changes for central heavy ion collisions at higher cm energies ( $\sqrt{s_{nn}} > 5$  GeV).<sup>66</sup> In such high energy domain, the nuclear matter, highly compressed as a result of head-on collision of heavy ions, undergoes a phase transition to a deconfined hot matter, called fireball, or Quark–Gluon Plasma (QGP), at energy density about 1 GeV/fm<sup>3</sup> and the temperature  $\sim 160$  MeV.<sup>66,68–70</sup> This threshold energy density for deconfinement was shown to be reached already at  $\sqrt{s_{nn}} \approx 5$  GeV from lattice QCD calculations.<sup>68</sup> This extremely dynamical event of a high energy central (head-on) nucleus–nucleus collision can schematically be described as undergoing the following stages<sup>66</sup>: (i) the initial collisions taking place

during the passage time of colliding nuclei ( $t_{\text{passage}} = 2R/(\gamma_{\text{cm}}c)$ ); (ii) establishment of equilibrium (thermalization); (iii) expansion and cooling of a fireball; (iv) chemical freeze-out (possibly at hadronization), when inelastic collisions cease and hadron yields (distribution over the species) are frozen; and (v) kinetic freeze-out, when elastic collisions cease, and particle spectra and correlations are fixed. In this case, it is natural that a significant fraction of cm energy is utilized for creation of the new particles. Obviously, the magnitude of spread around  $y_{\text{cm}} = 0$  of the rapidities of particles, originated from expansion and freeze-out of a fireball produced in central heavy ion collisions, and so the size of central rapidity region, increases significantly as compared to central nucleus–nucleus collisions at lower energies ( $\sqrt{s_{nn}} < 5$  GeV). For proton–proton collisions at ISR energies, the width of the central plateau region of rapidity distributions of particles, as well as their densities in the central region, increased with increasing  $\sqrt{s_{nn}}$ .<sup>35</sup>

In Ref. 18, the widths of rapidity distributions of particles produced in nucleus–nucleus collisions at various cm energies, and as a function of centrality at SPS energies, were studied. The rapidity distributions for pions from  $\sqrt{s_{nn}} = 2$  to 200 GeV were fitted with the thermal model function, which took into account a longitudinal flow. It was found that the average longitudinal velocity  $\langle\beta_L\rangle$  for pions increased with the cm energy, approaching a value of 1 at maximal RHIC energies from a value of 0.3 at AGS energies.<sup>18</sup> The width of rapidity distributions of particles in heavy ion collisions increased with increasing  $\sqrt{s_{nn}}$ . It was also observed that, at fixed  $\sqrt{s_{nn}}$ , the width of rapidity spectra in heavy ion collisions increased with the increase of impact parameter.<sup>18</sup> In Ref. 23, the widths of the cm rapidity distributions of the negative pions were extracted from fitting the pion spectra with a Gaussian given by

$$F(y) = \frac{A_0}{\sigma} \exp\left(\frac{-(y - y_0)^2}{2\sigma^2}\right), \quad (6)$$

where  $\sigma$  is the standard deviation, referred to as a width of distribution,  $y_0$  is the center of Gaussian distribution and  $A_0$  is the fitting constant. As shown in Ref. 23 and presented in Table 7, the increase of the width of rapidity distributions of the negative pions with increasing the collision impact parameter was observed also in  $^{12}\text{C}+^{12}\text{C}$  collisions at  $\sqrt{s_{nn}} = 3.14$  GeV.

Table 7. Parameters extracted in Ref. 23 from fitting by Gaussian function, given in expression (6), of the experimental cm rapidity distributions of the negative pions in minimum bias, central and peripheral  $^{12}\text{C}+^{12}\text{C}$  collisions at  $\sqrt{s_{nn}} = 3.14$  GeV.

Collision type	$A_0$	$\sigma$	$y_0$	$\chi^2/\text{n.d.f.}$	$R^2$
Minimum bias	$0.575 \pm 0.004$	$0.793 \pm 0.003$	$-0.016 \pm 0.005$	8.93	0.99
Central	$1.44 \pm 0.02$	$0.774 \pm 0.006$	$-0.021 \pm 0.009$	2.52	0.99
$\sim (0-10)\%$					
Peripheral	$0.274 \pm 0.003$	$0.813 \pm 0.006$	$-0.008 \pm 0.009$	2.76	0.99
$\sim (40-100)\%$					

The collective flow of protons and negative pions was also observed experimentally in He+C, C+C, C+Ne, C+Cu and C+Ta collisions at a momentum range of 4.2A–4.5A GeV/c.<sup>48,71,72</sup> One can have a rough estimate for an average width ( $\Delta y_{\text{centr}}$ ) of central rapidity region for pions coming from expansion and freeze-out of a compressed nuclear matter in central  $^{12}\text{C}+^{12}\text{C}$  collisions at  $\sqrt{s_{nn}} = 3.14$  GeV. As the longitudinal component of the collective flow of the particles, in the case of central symmetric collisions, expands simultaneously with the same  $\langle\beta_L\rangle$  to opposite longitudinal directions from the cm of collision system, the rough estimate for  $\Delta y_{\text{centr}}$  can be proposed as follows:

$$\Delta y_{\text{centr}} \approx 2 \left( \frac{1}{2} \ln \frac{1 + \langle\beta_L\rangle}{1 - \langle\beta_L\rangle} \right). \quad (7)$$

Using the graph of the  $\langle\beta_L\rangle$  versus  $\sqrt{s_{nn}}$  dependence, given in Ref. 18, we obtained a rough estimate  $\langle\beta_L\rangle \approx 0.4$  at  $\sqrt{s_{nn}} = 3.14$  GeV. Substituting this value into expression (7),  $\Delta y_{\text{centr}} \approx 0.85$  was obtained for the negative pions in  $^{12}\text{C}+^{12}\text{C}$  collisions at  $\sqrt{s_{nn}} = 3.14$  GeV. Interestingly, this estimate of  $\Delta y_{\text{centr}}$  for the negative pions proved to be close to the width ( $\sigma$ ) of rapidity distribution of  $\pi^-$  in central collisions extracted using Gaussian fits in Ref. 23, and shown in Table 7. On the other hand, the full width at half maximum (FWHM) of a Gaussian distribution given in (6) is approximately  $2.35\sigma$ . Using the width ( $\sigma$ ) extracted in Ref. 23 for central  $^{12}\text{C}+^{12}\text{C}$  collisions (given in Table 7), FWHM  $\approx 1.82$  was obtained. This value of FWHM came out to be close to the values of  $y_0$ , extracted in the present analysis, as seen in Tables 3 and 4.

The parameter  $\Delta$  in expression (4) could be ascribed to the quantity inversely proportional to the rate of fall off in the rapidity spectra in the fragmentation regions of the colliding nuclei. Indeed, by varying the  $\Delta$  value and keeping all the other parameters fixed, it can easily be verified from expression (4) that the normalized cm rapidity density decreases (the rate of fall off increases) with decreasing parameter  $\Delta$ .

Let us revert to the discussion of the factor  $(AA)^{f(y)}$  in expression (4). It can be assumed initially that, in symmetric central collisions with practically complete overlap of the two colliding identical nuclei, this factor accounts for the degree of involvement of all the constituent nucleons of the colliding nuclei in the creation of a compressed nucleonic matter, or highly excited nuclear matter, at lower energies ( $\sqrt{s_{nn}} < 5$  GeV) or production of a fireball (or QGP) at higher energies ( $\sqrt{s_{nn}} > 5$  GeV). As  $f(y) = \gamma y^2 (\beta = 0)$  is assumed in symmetric central collisions of identical nuclei, such degree of involvement of the constituent nucleons of colliding nuclei in central nucleus–nucleus collisions would be determined by the parameter  $\gamma$ . As seen from Table 5, the value of  $\gamma$  for the negative pions increased quite prominently with the increase of  $\sqrt{s_{nn}}$  from 6.3 to 12.3 GeV in central Pb+Pb collisions. As shown in Ref. 34, the value of  $\gamma$  for pions continued to increase with the cm energy even at higher RHIC energies in central Au+Au collisions between  $\sqrt{s_{nn}} = 19.6$  and 200 GeV, reaching the value  $\gamma = -0.00890 \pm 0.00003$  in central Au+Au collisions

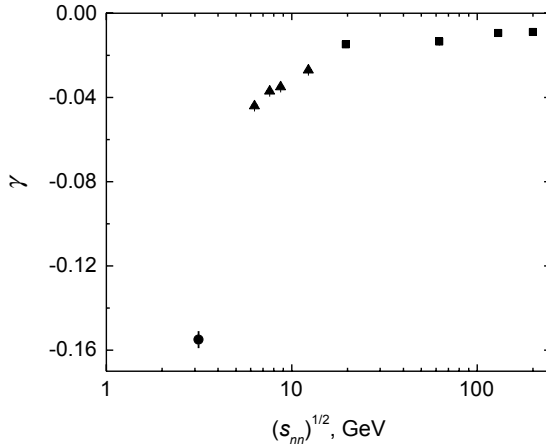


Fig. 3. Cm energy dependence of the parameter  $\gamma$  for pions, extracted in central  $^{12}\text{C}+^{12}\text{C}$  ( $\bullet$ ), central Pb+Pb<sup>34</sup> ( $\blacktriangle$ ), and central Au+Au<sup>34</sup> ( $\blacksquare$ ) collisions. The data presented correspond to  $\sim$  (0–10)% collision centrality.

at  $\sqrt{s_{nn}} = 200$  GeV. The cm energy dependence of the parameter  $\gamma$ , extracted for pions in central  $^{12}\text{C}+^{12}\text{C}$  collisions at  $\sqrt{s_{nn}} = 3.14$  GeV, central Pb+Pb collisions at  $\sqrt{s_{nn}}$  between 6.3 and 12.3 GeV, and central Au+Au collisions at  $\sqrt{s_{nn}}$  between 19.6 and 200 GeV, is presented in Fig. 3. The observed cm energy dependence of  $\gamma$  suggests its approximate ( $\gamma \rightarrow 0$  as  $\sqrt{s_{nn}} \rightarrow \infty$ ) asymptotic behavior.

It is important to mention that also the  $\gamma$ 's extracted for the other particles, such as charged kaons and  $\phi$ , produced in central collisions of identical heavy ions, revealed<sup>33,34</sup> the similar increasing trend with  $\sqrt{s_{nn}}$  and showed a tendency to approach approximately zero value asymptotically as  $\sqrt{s_{nn}} \rightarrow \infty$ . This can be observed from Fig. 4, which presents the cm energy dependence of the parameter  $\gamma$  extracted<sup>34</sup> for the negative pions,  $K^+$ ,  $K^-$  and  $\phi$  mesons from their experimental cm rapidity distributions in central Pb+Pb collisions at AGS and SPS energies.

As seen from Fig. 4, the gap between  $\gamma$ 's, extracted for pions and for the charged kaons and  $\phi$  mesons, reduced quite prominently with the increase of  $\sqrt{s_{nn}}$  from 6.3 to 12.3 GeV, and the  $\gamma$ 's for the charged kaons and  $\phi$  tended to approach that for the negative pions as  $\sqrt{s_{nn}}$  increased. The differences observed between the  $\gamma$ 's extracted for various particles and shown in Fig. 4 can be explained if the cm energy dependence of  $\gamma$  is related to the cm collision energy dependence of the particle yields at midrapidity ( $\frac{dN}{dy}|_{y_{cm}=0}$ ) and to the degree of dehadronization of a collision system in central collisions of identical heavy ions. The differences between  $\gamma$ 's for  $K^+$  and  $K^-$  can be explained by the differences between  $K^+$  and  $K^-$  meson yields at midrapidity at AGS and SPS energies, discussed in Ref. 66. The difference in yields is determined by the quark content of these hadrons,  $K^+(u\bar{s})$ , and  $K^-(\bar{u}s)$ . The availability in a fireball of valence  $u, d$  quarks from colliding nucleons

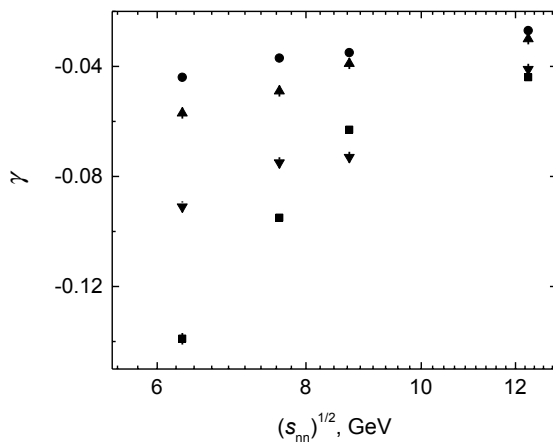


Fig. 4.  $\sqrt{s_{nn}}$  energy dependence of the parameter  $\gamma$  extracted<sup>34</sup> for the negative pions (●),  $K^+$  (▲),  $K^-$  (▼) and  $\phi$  mesons (■) from their experimental  $\sqrt{s_{nn}}$  rapidity distributions in central Pb+Pb collisions at AGS and SPS energies.

“stopped” in the fireball led to a preferential production of hadrons carrying these quarks.<sup>66</sup> These differences vanished at higher RHIC energies, where hadrons were mostly newly created and the production yielded a clear mass ordering.<sup>66</sup> This supports further the statement that both the degree of dehadronization and fraction of constituent nucleons of a collision system, which underwent transition into QGP, along with its energy density, increase as  $\sqrt{s_{nn}}$  increases in central heavy ion collisions at high energies. The differences in Fig. 4 between  $\gamma$  for  $\phi$  mesons and  $\gamma$ 's for the other particles can be explained by that the  $\phi$  meson ( $s\bar{s}$ ) requires production of both the strange quark and its antiparticle (much heavier than light  $u$  and  $d$  quarks), which are not available in the colliding nucleons.

It can easily be verified that, for  $\gamma \leq 0$  and finite rapidities, the factor  $(AA)^{\gamma y^2}$  reaches its maximum value 1 at  $\gamma = 0$ . Hence, it can be conjectured that  $\gamma \cong 0$  could possibly be related to the complete dehadronization of all the constituent nucleons of a collision system as a result of head-on collision of two identical nuclei, when the whole colliding system undergoes transformation into the state of deconfined quarks and gluons (QGP) and attains its highest possible energy density. At fixed  $\gamma$  ( $\gamma < 0$ ), the factor  $(AA)^{\gamma y^2}$  has its maximum value 1 at  $y_{cm} = 0$  and falls off rapidly as  $|y_{cm}|$  increases towards the fragmentation region of the colliding identical nuclei, which would mean asymptotically  $(AA)^{\gamma y^2} \rightarrow 0$  as  $|y_{cm}| \rightarrow \infty$ . While at  $\gamma = 0$ , the factor  $(AA)^{\gamma y^2}$  would retain its maximum value 1 in the whole  $\sqrt{s_{nn}}$  rapidity range of the produced particles, being independent of  $y_{cm}$ . Figure 3 shows a large gap between the values of  $\gamma$  for central  $^{12}\text{C}+^{12}\text{C}$  collisions at  $\sqrt{s_{nn}} = 3.14$  GeV and central Pb+Pb collisions at  $\sqrt{s_{nn}} \geq 6.3$  GeV. This is in line with the above mentioned lattice QCD calculations, predicting the threshold energy density for deconfinement phase transition to be reached already at  $\sqrt{s_{nn}} \approx 5$  GeV. Hence, the parameter  $\gamma$  could possibly be sensitive to deconfinement phase transition of a nuclear matter

and, as already argued, is possibly an indicator of degree of dehadronization of the whole collision system (or/and an indicator of the fraction of constituent nucleons of the collision system, which underwent transition into the QGP, and its energy density) in central collisions of identical nuclei. We believe that, due to the lowest threshold energy (among hadrons) of pion production (which requires only the lightest  $u$  and  $d$  quarks and their antiparticles), an initial onset of deconfinement transition could possibly be deduced from analysis of cm energy dependence of the relevant pion spectra and related phenomenological parameter(s). For more convincing evidence, one would possibly require 5–6 more experimental data points for  $\gamma$  extracted for pions in central collisions of identical nuclei at  $\sqrt{s_{nn}}$  between 3 and 6 GeV. Then, one could possibly identify and estimate the value of cm energy for an abrupt growth of  $\gamma$  in experiment, for a comparison with the existing theoretical expectations.

Due to the estimated threshold cm collision energy  $\sqrt{s_{nn}} \approx 5$  GeV, required for reaching the deconfinement threshold energy density, it is expected that quite large fraction of constituent nucleons of a collision system should undergo transition to QGP in central heavy ion collisions at  $\sqrt{s_{nn}} \geq 6.3$  GeV. This fraction as well as the energy density of QGP are expected to increase with increasing  $\sqrt{s_{nn}}$  in this high energy domain. Much smaller value of  $\gamma$  extracted for central  $^{12}\text{C}+^{12}\text{C}$  collisions at  $\sqrt{s_{nn}} = 3.14$  GeV than  $\gamma$ 's obtained in central heavy ion collisions at  $\sqrt{s_{nn}} \geq 6.3$  GeV could then be explained by a very small or practically zero degree of dehadronization of the constituent nucleons, and relatively small energy density, reached in central  $^{12}\text{C}+^{12}\text{C}$  collisions as compared to quite large fraction of constituent nucleons of a collision system, which underwent transition into QGP, and much higher energy densities attained in central Pb+Pb and Au+Au collisions at high energies.

Finally, it is of importance also to check an initial assumption that the parameter  $\beta$  in expression (4) should be fixed as  $\beta = 0$  due to a symmetry of collision system. For this, all the fits of the experimental and model spectra, presented in Figs. 1 and 2 and Tables 3 and 4, have been redone letting the parameter  $\beta$  to vary. The parameters extracted from  $\chi^2$  fitting by expression in (4) of the experimental and Modified FRITIOF model cm rapidity distributions of the negative pions for minimum bias, central and peripheral  $^{12}\text{C}+^{12}\text{C}$  collisions for the fixed  $\Delta = 0.55$  only, and allowing all the parameters to vary are presented in Tables 8 and 9, respectively. As observed from Tables 8 and 9, the extracted values of  $\beta$  came out to be essentially zero, within the uncertainties. This validates the initial assumption that  $\beta = 0$ , made on symmetry consideration, for the cm rapidity distributions of particles produced in collisions of identical nuclei. Comparing Tables 3 and 8 and Tables 4 and 9, one can see that the varying of the parameter  $\beta$  practically has no effect on and does not change appreciably any of the other extracted parameters, such as  $C, \gamma, y_0$  and  $\Delta$ .

Table 8. Parameters of approximation by the expression in (4) of the cm rapidity distributions of the negative pions in minimum bias, central and peripheral  $^{12}\text{C}+^{12}\text{C}$  collisions at  $\sqrt{s_{nn}} = 3.14$  GeV ( $\Delta = 0.55$  is fixed).

Collision type	Type	$C$	$\beta$	$\gamma$	$y_0$	$\chi^2/\text{n.d.f.}$	$R^2$
Minimum bias	Experiment	$0.73 \pm 0.02$	$-0.005 \pm 0.002$	$-0.13 \pm 0.03$	$2.07 \pm 0.69$	5.34	0.99
	Mod. = Modified FRITIOF	$0.76 \pm 0.02$	$-0.006 \pm 0.001$	$-0.15 \pm 0.02$	$2.01 \pm 0.55$	6.35	0.99
Central $\sim (0-10)\%$	Experiment	$1.86 \pm 0.07$	$-0.007 \pm 0.003$	$-0.14 \pm 0.04$	$2.16 \pm 1.08$	1.82	0.99
	Mod. = Modified FRITIOF	$1.80 \pm 0.10$	$-0.005 \pm 0.002$	$-0.15 \pm 0.04$	$2.03 \pm 1.11$	1.80	0.99
Peripheral $\sim (40-100)\%$	Experiment	$0.34 \pm 0.03$	$-0.002 \pm 0.003$	$-0.12 \pm 0.06$	$2.00 \pm 1.50$	1.85	0.99
	Mod. = Modified FRITIOF	$0.44 \pm 0.02$	$-0.002 \pm 0.002$	$-0.14 \pm 0.04$	$2.00 \pm 0.91$	4.10	0.99

Table 9. Parameters of approximation by the expression in (4) of the cm rapidity distributions of the negative pions in minimum bias, central and peripheral  $^{12}\text{C}+^{12}\text{C}$  collisions at  $\sqrt{s_{nn}} = 3.14$  GeV.

Collision type	Type	$C$	$\beta$	$\gamma$	$y_0$	$\Delta$	$\chi^2/\text{n.d.f.}$	$R^2$
Minimum bias	Experiment	$0.69 \pm 0.01$	$-0.005 \pm 0.002$	$-0.141 \pm 0.003$	$2.23 \pm 0.05$	$0.22 \pm 0.03$	2.38	0.99
	Mod. = Modified FRITIOF	$0.72 \pm 0.01$	$-0.006 \pm 0.001$	$-0.154 \pm 0.005$	$2.12 \pm 0.08$	$0.32 \pm 0.04$	3.41	0.99
Central $\sim (0-10)\%$	Experiment	$1.79 \pm 0.03$	$-0.008 \pm 0.003$	$-0.155 \pm 0.003$	$2.33 \pm 0.05$	$0.10 \pm 0.04$	0.87	0.99
	Mod. = Modified FRITIOF	$1.73 \pm 0.02$	$-0.005 \pm 0.002$	$-0.167 \pm 0.007$	$2.28 \pm 0.11$	$0.29 \pm 0.09$	1.55	0.99
Peripheral $\sim (40-100)\%$	Experiment	$0.32 \pm 0.01$	$-0.0005 \pm 0.003$	$-0.127 \pm 0.008$	$2.10 \pm 0.11$	$0.26 \pm 0.06$	0.98	0.99
	Mod. = Modified FRITIOF	$0.41 \pm 0.01$	$-0.001 \pm 0.002$	$-0.147 \pm 0.007$	$2.04 \pm 0.09$	$0.29 \pm 0.04$	1.78	0.99

#### 4. Summary and Conclusions

The experimental cm rapidity distributions of the negative pions in  $^{12}\text{C}+^{12}\text{C}$  collisions at  $4.2A\text{ GeV}/c$  ( $\sqrt{s_{nn}} = 3.14\text{ GeV}$ ) were described quite satisfactorily using the simple phenomenological model, the GCM. Similar analysis was made for the cm rapidity distributions of the negative pions, calculated using Modified FRITIOF model, in  $^{12}\text{C}+^{12}\text{C}$  collisions at  $\sqrt{s_{nn}} = 3.14\text{ GeV}$ . The GCM parameters extracted from fitting the cm rapidity distributions of the negative pions in central  $^{12}\text{C}+^{12}\text{C}$  collisions were compared with the corresponding parameters extracted earlier for pions produced in central Pb+Pb collisions at SPS and AGS energies between  $\sqrt{s_{nn}} = 6.3\text{ GeV}$  and  $\sqrt{s_{nn}} = 12.3\text{ GeV}$  and in central Au+Au collisions at RHIC energies from  $\sqrt{s_{nn}} = 19.6\text{ GeV}$  to  $200\text{ GeV}$ .

By letting the parameter  $\beta$  to vary, the initial assumption that  $\beta = 0$  in expression (4), made on symmetry consideration, for the cm rapidity distributions of particles produced in collisions of identical nuclei was validated. The extracted values of  $\beta$  came out to be practically zero and did not change appreciably any of the other extracted parameters, such as  $C$ ,  $\gamma$ ,  $y_0$  and  $\Delta$ . The ratio of the fitting constants  $C$ , given in expression (4), in central and peripheral  $^{12}\text{C}+^{12}\text{C}$  collisions agreed within the uncertainties with the ratio of the mean multiplicities of the negative pions in central and peripheral collisions, both in the experiment and model. This result showed that the fitting constant  $C$  in expression (4) fixes the multiplicity of the studied particles. Parameters  $y_0(\gamma)$  and  $\Delta$  showed some noticeable correlation, i.e.,  $y_0(\gamma)$  decreased (increased) weakly with the increase of  $\Delta$ . It was deduced that  $y_0$  was likely to be a quantity related to a maximum rapidity spread (around central rapidity region) of particles originated from expansion and freeze-out of a fireball. A rough estimate for the average size of central rapidity region for the negative pions in central  $^{12}\text{C}+^{12}\text{C}$  collisions was obtained to be  $\Delta y_{\text{centr}} \approx 0.85$ , using  $\langle\beta_L\rangle \approx 0.4$  at  $\sqrt{s_{nn}} = 3.14\text{ GeV}$  extracted from the graph of  $\langle\beta_L\rangle$  versus  $\sqrt{s_{nn}}$  dependence, given in Ref. 18. This value of  $\Delta y_{\text{centr}}$  for the negative pions proved to be close to the width ( $\sigma$ ) of rapidity distribution of  $\pi^-$  in central  $^{12}\text{C}+^{12}\text{C}$  collisions extracted using Gaussian fit in Ref. 23. The extracted values of  $y_0$  proved to be close to the FWHM  $\approx 1.82$  ( $2.35\sigma$ ) of rapidity distribution of the negative pions in  $^{12}\text{C}+^{12}\text{C}$  collisions. The parameter  $\Delta$  could be associated with the quantity inversely proportional to the rate of fall off in the rapidity spectra in fragmentation regions of colliding nuclei.

The parameter  $\gamma$  in the  $(AA)^{\gamma y^2}$  factor could possibly be an indicator of a degree of dehadronization of all the constituent nucleons of collision system and its energy density attained in central collisions of identical nuclei. Its approximate ( $\gamma \rightarrow 0$  as  $\sqrt{s_{nn}} \rightarrow \infty$ ) asymptotic behavior was deduced from analysis of cm energy dependence of  $\gamma$ , extracted for pions in central  $^{12}\text{C}+^{12}\text{C}$  collisions at  $\sqrt{s_{nn}} = 3.14\text{ GeV}$ , central Pb+Pb collisions at  $\sqrt{s_{nn}}$  between 6.3 and 12.3 GeV and central Au+Au collisions at  $\sqrt{s_{nn}}$  between 19.6 and 200 GeV. The  $\gamma$ 's extracted earlier for the other particles, such as kaons and  $\phi$ , produced in central Pb+Pb collisions,

also revealed the similar increasing behavior with the  $\sqrt{s_{nn}}$  and showed a tendency to approach approximately zero value asymptotically as  $\sqrt{s_{nn}} \rightarrow \infty$ . For  $\gamma \leq 0$  and finite rapidities, the factor  $(AA)^{\gamma y^2}$  attains its maximum value 1 at  $\gamma = 0$ . Physically,  $\gamma \cong 0$  could possibly be related to complete dehadronization of all the constituent nucleons of the collision system as a result of head-on collision of two identical nuclei, when the whole colliding system undergoes transformation into the state of free (deconfined) quarks and gluons, and attains its highest possible energy density. A large gap was observed between the values of  $\gamma$  for central  $^{12}\text{C}+^{12}\text{C}$  collisions at  $\sqrt{s_{nn}} = 3.14$  GeV and central Pb+Pb collisions at  $\sqrt{s_{nn}} \geq 6.3$  GeV. This was in line with the theoretical expectation<sup>68</sup> that the critical energy density for transition of a nuclear matter into the phase of deconfined quarks and gluons should reach already at  $\sqrt{s_{nn}} \approx 5$  GeV. Hence, the parameter  $\gamma$  could possibly be sensitive to deconfinement phase transition. For more convincing evidence, one would possibly require 5–6 more experimental data points for  $\gamma$  extracted for pions in central collisions of identical nuclei at  $\sqrt{s_{nn}}$  between 3 and 6 GeV. This could help to possibly identify and estimate the value of cm energy for an abrupt growth of  $\gamma$  in experiment, for comparison with the existing theoretical expectations. Much smaller value of  $\gamma$  extracted in central  $^{12}\text{C}+^{12}\text{C}$  collisions at  $\sqrt{s_{nn}} = 3.14$  GeV than  $\gamma$ 's obtained in central heavy ion collisions at  $\sqrt{s_{nn}} \geq 6.3$  GeV could be explained as follows. Very little or practically zero degree of dehadronization of constituent nucleons with relatively low energy density is expected in central  $^{12}\text{C}+^{12}\text{C}$  collisions at  $\sqrt{s_{nn}} = 3.14$  GeV as compared to quite large degree of dehadronization of the whole collision system with much higher energy densities attained in central Pb+Pb and Au+Au collisions at high energies.

### Acknowledgments

We are grateful to the staff of Laboratory of High Energies of JINR (Dubna, Russia) and of Laboratory of Multiple Processes of Physical-Technical Institute of Uzbek Academy of Sciences (Tashkent, Uzbekistan) for processing the stereophotographs from 2 m propane bubble chamber of JINR. We thank V. V. Uzhinskii and A. S. Galoyan (JINR, Dubna) for providing us the code of Modified FRITIOF model. Q. Ali, M. Q. Haseeb and A. Arif acknowledge the partial support from HEC Research Project No. 1925.

### References

1. P. Braun-Munzinger and J. Stachel, *Annu. Rev. Nucl. Part. Sci.* **37** (1987) 97.
2. R. Stock *et al.*, *Phys. Rev. Lett.* **49** (1982) 1236.
3. Kh. K. Olimov, Mahnaz Q. Haseeb, Imran Khan, A. K. Olimov and V. V. Glagolev, *Phys. Rev. C* **85** (2012) 014907.
4. Kh. K. Olimov, M. Q. Haseeb and I. Khan, *Phys. At. Nucl.* **75** (2012) 479.
5. Kh. K. Olimov *et al.*, *Phys. Rev. C* **75** (2007) 067901.
6. Kh. K. Olimov and M. Q. Haseeb, *Eur. Phys. J. A* **47** (2011) 79.

7. Kh. K. Olimov, M. Q. Haseeb, A. K. Olimov and I. Khan, *Cent. Eur. J. Phys.* **9** (2011) 1393.
8. D. Krpic, G. Skoro, I. Picuric, S. Backovic and S. Drndarevic, *Phys. Rev. C* **65** (2002) 034909.
9. Kh. K. Olimov, *Phys. Rev. C* **76** (2007) 055202.
10. Kh. K. Olimov, S. L. Lutpullaev, B. S. Yuldashev, Y. H. Huseynaliyev and A. K. Olimov, *Eur. Phys. J. A* **44** (2010) 43.
11. Kh. K. Olimov, *Phys. At. Nucl.* **73** (2010) 433.
12. B.-A. Li and C. M. Ko, *Phys. Rev. C* **52** (1995) 2037.
13. W. Ehehalt, W. Cassing, A. Engel, U. Mosel and Gy. Wolf, *Phys. Lett. B* **298** (1993) 31.
14. FOPI Collab. (M. Eskef et al.), *Eur. Phys. J. A* **3** (1998) 335.
15. E814 Collab. (J. Barrette et al.), *Phys. Lett. B* **351** (1995) 93.
16. G. E. Brown, J. Stachel and G. M. Welke, *Phys. Lett. B* **253** (1991) 19.
17. B.-A. Li and W. Bauer, *Phys. Rev. C* **44** (1991) 450.
18. P. K. Netrakanti and B. Mohanty, *Phys. Rev. C* **71** (2005) 047901.
19. Lj. Simic et al., *Phys. Rev. C* **52** (1995) 356.
20. R. N. Bekmirzaev, E. N. Kladnitskaya and S. A. Sharipova, *Phys. At. Nucl.* **58** (1995) 58.
21. R. N. Bekmirzaev, E. N. Kladnitskaya, M. M. Muminov and S. A. Sharipova, *Phys. At. Nucl.* **58** (1995) 1721.
22. L. Chkhaidze, T. Djobava, L. Kharkhelaury and M. Mosidze, *Eur. Phys. J. A* **1** (1998) 299.
23. Kh. K. Olimov, A. Iqbal, V. V. Glagolev and M. Q. Haseeb, *Phys. Rev. C* **88** (2013) 064903.
24. E895 Collab. (J. L. Klay et al.), *Phys. Rev. Lett.* **88** (2002) 102301.
25. J. Aichelin and K. Werner, *Phys. Lett. B* **300** (1993) 158.
26. B. Mohanty and J. Alam, *Phys. Rev. C* **68** (2003) 064903.
27. Kh. K. Olimov and M. Q. Haseeb, *Phys. At. Nucl.* **76** (2013) 595.
28. A. Iqbal et al., *Int. J. Mod. Phys. E* **23** (2014) 1450047.
29. Kh. K. Olimov et al., *Int. J. Mod. Phys. E* **23** (2014) 1450084.
30. Kh. K. Olimov, M. Q. Haseeb and S. A. Hadi, *Int. J. Mod. Phys. E* **22** (2013) 1350020.
31. B. De and S. Bhattacharyya, *Int. J. Mod. Phys. A* **19** (2004) 2313.
32. B. De, S. Bhattacharyya and P. Guptaroy, *Int. J. Mod. Phys. A* **17** (2002) 4615.
33. G. Sau et al., *Nuovo Cimento B* **125** (2010) 833.
34. G. Sau et al., *J. Mod. Phys.* **2** (2011) 1354.
35. W. Thome et al., *Nucl. Phys. B* **129** (1977) 365.
36. M. A. Faessler, *Phys. Rep.* **115** (1984) 1.
37. H. R. Schmidt and J. Schukraft, *J. Phys. G, Nucl. Part. Phys.* **19** (1993) 1705.
38. T. Peitzmann, *Phys. Lett. B* **450** (1999) 7.
39. B. Gankhuyag and V. V. Uzhinskii, Modified FRITIOF code: Negative charged particle production in high-energy nucleus-nucleus interactions, JINR Preprint No. P2-96-419 (Dubna, 1996).
40. A. S. Galoyan, G. L. Melkumov and V. V. Uzhinskii, *Phys. At. Nucl.* **65** (2002) 1722.
41. A. I. Bondarenko et al., *Phys. At. Nucl.* **65** (2002) 90.
42. A. S. Galoyan et al., *Phys. At. Nucl.* **66** (2003) 836.
43. G. N. Agakishiyev et al., *Z. Phys. C* **27** (1985) 177.
44. D. Armutlisky et al., *Z. Phys. A* **328** (1987) 455.
45. A. I. Bondarenko et al., The Ensemble of interactions on carbon and hydrogen nuclei obtained using the 2 m propane bubble chamber exposed to the beams of protons and

- H-2, He-4, C-12 relativistic nuclei at the Dubna Synchrophasotron.”, JINR Preprint No. P1-98-292 (JINR, Dubna, 1998).
46. L. Chkhaidze, T. Djobava and L. Kharkhelaury, *Bull. Georg. Natl. Acad. Sci.* **6** (2012) 44.
  47. K. Olimov, S. L. Lutpullaev, A. K. Olimov, V. I. Petrov and S. A. Sharipova, *Phys. At. Nucl.* **73** (2010) 1847.
  48. L. Chkhaidze, P. Danielewicz, T. Djobava, L. Kharkhelaury and E. Kladnitskaya, *Nucl. Phys. A* **794** (2007) 115.
  49. A. I. Bondarenko *et al.*, *Phys. At. Nucl.* **60** (1997) 1833.
  50. Ts. Baatar *et al.*, *Phys. At. Nucl.* **63** (2000) 839.
  51. B. Andersson *et al.*, *Nucl. Phys. B* **281** (1987) 289.
  52. B. Nilsson-Almqvist and E. Stenlund, *Comput. Phys. Commun.* **43** (1987) 387.
  53. B. Gankhuyag and V. V. Uzhinskii, JINR Communications No. P1-97-315 (Dubna, 1997).
  54. B. Gankhuyag and V. V. Uzhinskii, JINR Communications No. P2-97-397 (Dubna, 1997).
  55. K. El-Waged and V. V. Uzhinskii, *Phys. At. Nucl.* **60** (1997) 828.
  56. S. Yu. Shmakov, V. V. Uzhinskii and A. M. Zadorojny, *Comput. Phys. Commun.* **54** (1989) 125.
  57. EMU-01 Collab. (M. I. Adamovich *et al.*), *Z. Phys. A* **358** (1997) 337.
  58. V. Weisskopf, *Phys. Rev.* **52** (1937) 295.
  59. V. S. Barashenkov and V. D. Toneev, *Interactions of High-Energy Particles and Atomic Nuclei with Nuclei* (Atomizdat, Moscow, 1972).
  60. V. V. Uzhinskii and S. Yu. Shmakov, *Phys. At. Nucl.* **57** (1994) 1459.
  61. S. Backovic *et al.*, *Sov. J. Nucl. Phys.* **50** (1989) 1001.
  62. J. Benecke *et al.*, *Phys. Rev.* **188** (1969) 2159.
  63. R. P. Feynmann, *Phys. Rev. Lett.* **23** (1969) 1415.
  64. S. Bhattacharyya, *Lett. Nuovo Cimento* **44** (1985) 119.
  65. R. C. Hwa *et al.*, *Phys. Rev. C* **64** (2001) 054611.
  66. A. Adronic, *Int. J. Mod. Phys. A* **29** (2014) 1430047.
  67. G. F. Chapline *et al.*, *Phys. Rev. D* **8** (1973) 4302.
  68. F. Karsch, *Lect. Notes Phys.* **583** (2002) 209.
  69. Y. Aoki *et al.*, *J. High Energy Phys.* **0906** (2009) 088.
  70. A. Bazavov *et al.*, *Phys. Rev. D* **85** (2012) 054503.
  71. L. Chkhaidze *et al.*, *Phys. Rev. C* **84** (2011) 064915.
  72. L. V. Chkhaidze *et al.*, *Phys. At. Nucl.* **67** (2004) 693.